

1 **Title:** Mississippi River low-flows: context, causes, and future projections
2 **Authors:** Samuel E. Muñoz^{1,2}, Sylvia G. Dee³, Xinyue Luo³, M. Rezaul Haider³, Michelle
3 O'Donnell², B. Parazin¹, Jonathan W.F. Remo⁴

4
5 ¹Department of Marine & Environmental Sciences, Northeastern University, Marine Science
6 Center, Nahant MA, USA

7 ²Department of Civil & Environmental Engineering, Northeastern University, Boston MA, USA

8 ³Department of Earth, Environmental, and Planetary Sciences, Rice University, Houston TX,
9 USA

10 ⁴School of Earth Systems and Sustainability, Southern Illinois University, Carbondale IL, USA

11
12 **Corresponding author:** Samuel Muñoz (s.munoz@northeastern.edu)

13 **Keywords**

14 Mississippi River, drought, climate change, CESM2, El Niño-Southern Oscillation, La Niña

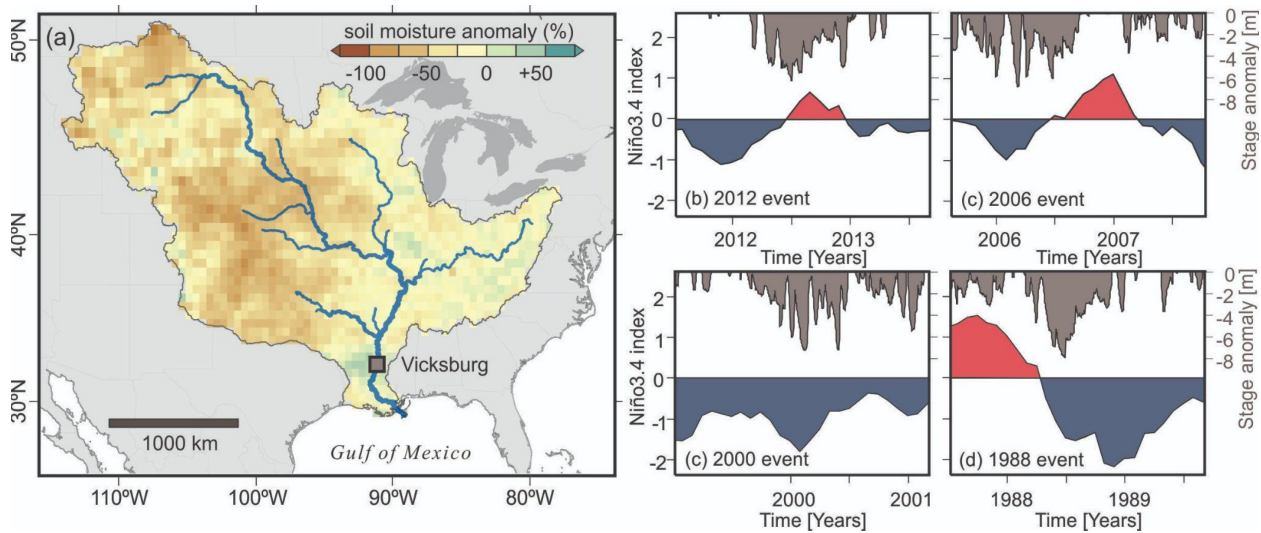
15 **Abstract**

16 The Mississippi River represents a major commercial waterway, and periods of anomalously low
17 river levels disrupt riverine transport. These low-flow events occur periodically, with a recent
18 event in the fall of 2022 slowing barge traffic and generating sharp increases in riverine
19 transportation costs. Here we combine instrumental river gage observations from the lower
20 Mississippi River with output from the Community Earth System Model v2 (CESM2) Large
21 Ensemble (LENS2) to evaluate historical trends and future projections of Mississippi River low
22 streamflow extremes, place the 2022 low-flow event in a broader temporal context, and assess
23 the hydroclimatic mechanisms that mediate the occurrence of low-flows. We show that the
24 severity and duration of low-flow events gradually decreased between 1950–1980 coincident
25 with the establishment of artificial reservoirs. In the context of the last ~70 years, the 2022 low-
26 flow event was less severe in terms of stage or discharge minima than other low-flow events of
27 the mid- and late-20th century. Model simulations from the LENS2 dataset show that, under a
28 moderate-high emissions scenario (SSP3-7.0), the severity and duration of low-flow events is
29 projected to decrease through to the end of the 21st century. Finally, we use the large sample
30 size afforded by the LENS2 dataset to show that low-flow events on the Mississippi River are
31 associated with cold tropical Pacific forcing (i.e., La Niña conditions), providing support for the
32 hypothesis that the El Niño-Southern Oscillation (ENSO) plays a critical role in mediating
33 Mississippi River discharge extremes. We anticipate that our findings describing the trends in
34 and hydroclimatic mechanisms of Mississippi River low-flow occurrence will aid water resource
35 managers to reduce the negative impacts of low water levels on riverine transport.

36 **1 Introduction**

37 On the world's major river systems, periods of anomalously low river discharge or stage are
38 economically costly, and reflect the combined effects of hydrological drought, geomorphic
39 processes, and river management practices (Smakhtin 2001). In the fall of 2022, the
40 Mississippi River experienced one such low-flow event (Fig. 1a), where low river levels slowed

41 barge traffic and resulted in sharp increases in downbound grain barge rates (USDA 2022;
 42 USDOT 2022). The Mississippi River and its major tributaries represent an economically critical
 43 waterway that is federally managed to facilitate navigation and mitigate flooding using a system
 44 of levees, river training structures, spillways, and dams known as the Mississippi River and
 45 Tributaries (MR&T) project (Camillo and Pearcy 2004). Despite the implementation of these
 46 management efforts in the mid-20th century, low-flow events remain disruptive and occur
 47 periodically (Remo *et al* 2018; Turner 2022), with other notable low-flow events in 2012, 2006,
 48 2000, and 1988 (Fig. 1b-d). As part of this study, we investigate how the 2022 low-flow event
 49 compares to other historical events, and assess historical trends in the severity and duration of
 50 low-flows.



51
 52 **Figure 1.** Recent Mississippi River low-flows in relation to soil moisture and El Niño-Southern
 53 Oscillation (ENSO): (a) Mississippi River basin soil moisture anomalies in September 2022
 54 (Climate Prediction Center [CPC] Soil Moisture V2; Fan and van den Dool 2004) and location of
 55 Vicksburg, Mississippi stream gage; River stage anomalies in relation to Niño3.4 index during
 56 historic low-flow events in (b) 2012, (c) 2006, (d) 2000, and (e) 1988.

57 In addition to management, climate variability and change also mediate the discharge of the
 58 Mississippi River and its tributaries via their influence on precipitation, soil moisture, and
 59 evapotranspiration (Mallakpour and Villarini 2016; Muñoz and Dee 2017; Muñoz *et al* 2018; van
 60 der Wiel *et al* 2018; Wiman *et al* 2021; Luo *et al* 2023). Interannual variations in discharge and
 61 flood hazard of the lower Mississippi River are strongly influenced by the El Niño-Southern
 62 Oscillation (ENSO), where El Niño events are associated with positive soil moisture and
 63 discharge anomalies that result in enhanced flood hazard (Chen and Kumar 2002; Muñoz and
 64 Dee 2017; Muñoz *et al* 2023) — particularly during eastern Pacific El Niño events (Luo *et al*
 65 2023). Historical low-flow events correspond to periods of anomalously low soil moisture within
 66 the Mississippi River basin and are often preceded by La Niña events (Fig. 1), although the
 67 small sample size associated with the observational period precludes a robust statistical
 68 assessment of how ENSO mediates the occurrence of low-discharge events (Fig. S1).
 69 Attribution of greenhouse forcing on Mississippi River discharge also remains difficult to
 70 evaluate due to the competing roles of climate change, land use change, and MR&T project
 71 infrastructure on regional hydrology (Pinter *et al* 2008; Remo *et al* 2009; St. George 2018;

72 Dunne *et al* 2022), as historical and projected trends in river discharge extremes are sensitive to
73 river engineering and emissions scenarios (Tao *et al* 2014; van der Wiel *et al* 2018; Munoz *et al*
74 2018; Dunne *et al* 2022]. This study uses ensemble earth system model simulations to evaluate
75 the roles of both internal climate variability and external forcing on the severity, duration, and
76 timing of low-flows on the lower Mississippi River.

77 Here we combine observations from instrumental river gage records with output from an earth
78 system model to evaluate historical trends and future projections of Mississippi River low
79 streamflow extremes, and assess the hydroclimatic mechanisms that mediate the occurrence of
80 low-flows. We focus our analyses on the lower Mississippi River at Vicksburg (USGS ID
81 07289000) after 1950 to encompass the period when contemporary river management practices
82 and infrastructure of the MR&T project were expanded (1950–1980) and established (1980–
83 present) (Smith and Winkley 1996; Remo *et al* 2018). We first examine trends in observed
84 annual stage and discharge minima from 1950–2022, and then use output from the recently
85 published Community Earth System Model version 2 (CESM2) Large Ensemble (LENS2) to
86 examine historical and projected trends (1950–2100) in river runoff, soil moisture, and sea
87 surface temperatures under the SSP3-7.0 future emissions scenario (Danabasoglu *et al* 2020;
88 Rodgers *et al* 2021). The CESM2 LENS2 simulations do not simulate the influence of reservoirs
89 or other river management infrastructure, allowing us to test hypotheses concerning the drivers
90 of historical and projected changes in low-flows. Finally, the ensemble model simulations of sea
91 surface temperature and soil moisture anomalies are used to evaluate the role of internal
92 climate variability on low-flow occurrence.

93 2 Methods

94 2.1 Instrumental stream gage data

95 To evaluate observed trends in lower Mississippi River stages and discharge, daily stage and
96 discharge data were compiled for water years 1950 through 2022 for the stream gage at
97 Vicksburg, Mississippi (USGS ID 07289000). For the period 1950 through 2014, these data
98 were obtained directly from the United States Army Corps of Engineers (USACE). Daily
99 discharge and stage data for the period 2015 through 2022 were obtained from the United
100 States Geological Survey (USGS) National Water Dashboard (USGS 2022) and the USACE
101 Hydrologic Database (USACE 2022), respectively. From these daily stage and discharge data,
102 we computed the annual mean, minima, and maxima for each water year, as well as the
103 number of days in a water year where stages were <1.5 m (i.e., low-stage duration). We use the
104 threshold of <1.5 m because it is consistent with the low water reference (5 feet) used by the
105 National Oceanic and Atmospheric Administration (NOAA) at the Vicksburg gage; the low water
106 reference is defined as a stage low enough to cause impacts to commerce and shipping..

107 2.2 Reanalysis datasets

108 To examine historical patterns of soil moisture and sea surface temperature anomalies
109 associated with low-flow events, we use the Extended Reconstructed Sea Surface Temperature
110 v5 (ERSST v5; Huang *et al* 2017) and Climate Prediction Center (CPC) Soil Moisture (Fan and
111 van den Dool 2004) reanalysis products. We computed the Niño3.4 index in the 18 months

112 before and after historic low-flow events in 2012, 2006, 2000, and 1988 from the ERSST
113 dataset following Munoz and Dee (2017). We also examined the full sea surface temperature
114 anomaly field for the month of these events as well as events in 1977, 1964, and 1954, where
115 anomalies are computed based on the long-term climatological mean for the period 1950–2021.
116 We also computed a composite mean sea surface temperature anomaly for all events and
117 tested the significance of the anomalies using bootstrapping of the full ERSST dataset for the
118 period 1950–2021 with $n=10,000$ iterations. We also examined soil moisture anomalies within
119 the Mississippi River basin for the same low-flow events using a similar procedure as above,
120 and express these anomalies as percent differences from the long-term climatological mean.

121 2.3 Ensemble model simulations

122 We employ open source, fully-coupled large ensemble numerical climate simulations from the
123 Community Earth System Model version 2 (CESM2), a state-of-the-art general circulation model
124 (GCM) developed at the National Center for Atmospheric Research (Danabasoglu *et al* 2020;
125 Rodgers *et al* 2021). The Large Ensemble dataset of CESM2, LENS2, contains a 100-member
126 Large Ensemble at $\sim 1^\circ$ horizontal resolution for the period 1850–2014 based on historical
127 radiative forcing, and the same number of members for the future climate (2015–2100) using
128 the SSP3-7.0 radiative forcing scenario (Rodgers *et al* 2021). In this study, we employed the 50-
129 member sub-ensembles based on the original CMIP6 biomass burning emissions protocol. A
130 runoff routing model known as the Model for Scale Adaptive River Transport (MOSART), is
131 integrated into CESM2 via the Community Land Model version 5 (CLM5, (Lawrence *et al* 2019),
132 and simulates river discharge through the downslope routing of water from surface runoff,
133 subsurface runoff, and tributaries using a horizontal spatial resolution of $\sim 0.5^\circ$ although
134 hydrography and related inputs are at higher resolution (Li *et al* 2015). Importantly, MOSART
135 does not directly simulate the effects of reservoir operation, surface water withdrawal,
136 groundwater pumping, and irrigation on river discharge, so we use simulated discharge to
137 evaluate the role of climate variability and change on low-flows. River discharge simulated by
138 MOSART reproduces the seasonality and magnitude of the Mississippi River (Fig. S2) as well
139 as other large rivers reasonably well (Li *et al* 2015), and represents an improvement from the
140 River Transport Model (RTM) integrated into CESM1 used in prior work investigating the role of
141 climate variability and change on Mississippi River streamflow (Branstetter 2001; Munoz and
142 Dee, 2017; Wiman *et al* 2021; Dunne *et al* 2022).

143 From the LENS2 simulations, we extracted daily river discharge (QCHANR, m^3/s), sea surface
144 temperature (SST, $^\circ\text{K}$), and soil moisture (SOILLIQ, kg/m^2) for subsequent analysis. For
145 QCHANR, we extracted data from the model grid cell closest to Vicksburg (32.315°N ,
146 90.906°W). We then computed the annual minimum and mean for each simulated water year of
147 each ensemble member, extracted the day that annual minima occurred, and calculated the
148 ensemble mean. We also computed the 1%, 5%, and 10% lowest discharge events for each
149 ensemble member based on a quantile analysis, and used these quantiles to calculate low-flow
150 event duration and the relationships between low discharge events, soil moisture, and sea
151 surface temperatures. The timing of low-flows was used to extract sea surface temperature and
152 soil moisture patterns during and in the months prior to low-flow events; composite averages
153 maps and time series were produced to examine these patterns.

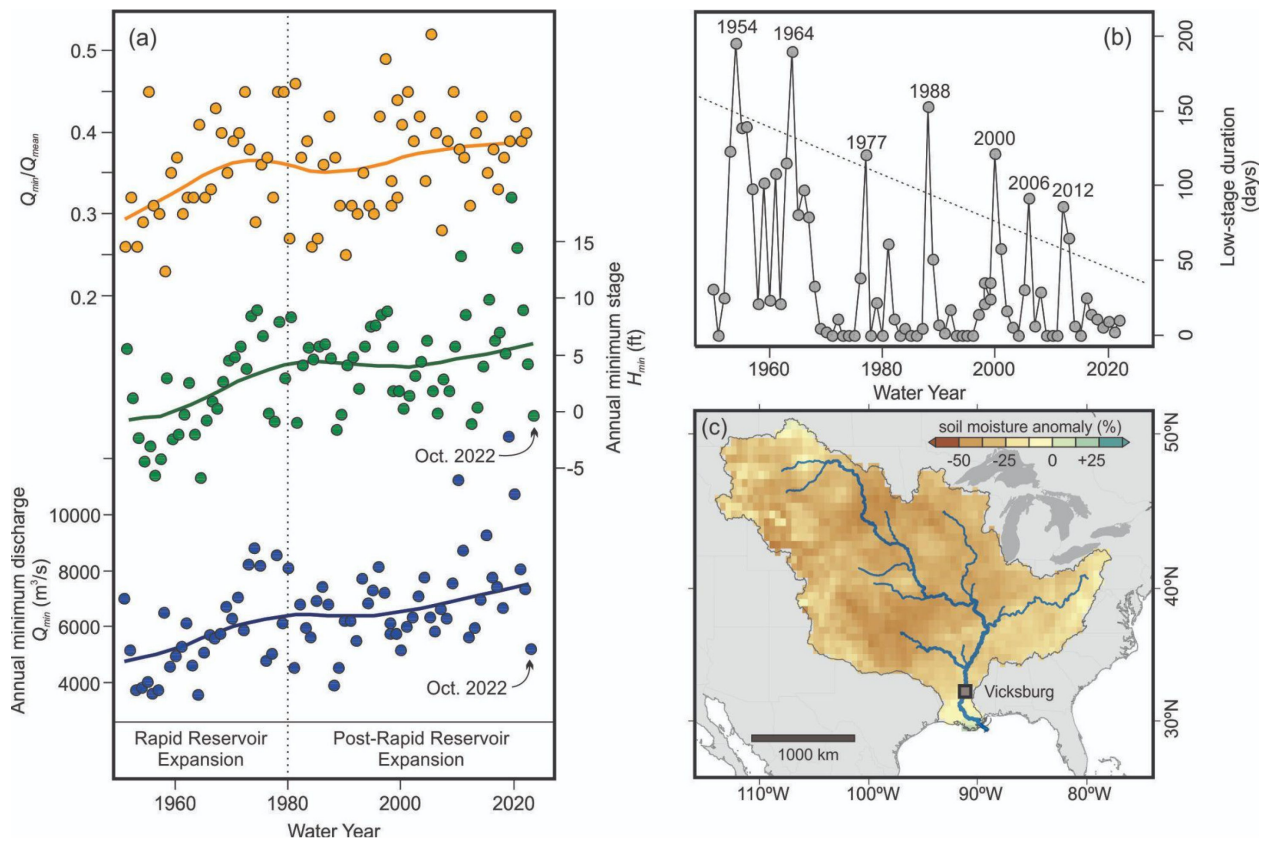
154
155 Finally, we employed an unsupervised machine learning method known as Self Organizing
156 Maps (SOMs) to detect shifts in the frequency of sea surface temperature patterns in the
157 LENS2 simulations before and after low-flow events on the lower Mississippi River. The SOM
158 method allows us to examine tropical Pacific sea surface temperature anomalies associated
159 with low-flow events in both time and space. The SOM method preserves the underlying data
160 structure of high-dimensional data while projecting it into two-dimensional space. Each annual
161 sea surface temperature anomaly pattern is classified to a best-fit SOM node which minimizes
162 the Euclidean distance between the actual year's sea surface temperature pattern and a
163 predefined set of SOM nodes. (Kohonen 1990; Liu *et al* 2006; Johnson *et al* 2008; Liu and
164 Weisberg 2011). Here we use six nodes because, based on our prior work where we conducted
165 sensitivity analyses using different numbers of nodes (Dee and Steiger, 2022; Luo *et al.* 2023),
166 we found that six nodes maximized the number of meaningful SOMs produced, while assigning
167 fewer nodes did not fully capture observed variability in tropical Pacific sea surface temperature
168 patterns. Sea surface temperature fields were pre-processed prior to applying the SOM
169 algorithm by detrending (i.e., removal of the 100-year smoothed time series; Horton *et al* 2015),
170 and area-weighting by the cosine of latitude. Finally, we perform a simple frequency analysis for
171 each sea surface temperature pattern during low-flow years (lowest 1% and 10% discharge
172 quantiles) and 'normal' years (25-75% discharge quantiles). To test the significance of
173 frequency shifts in the SOM patterns, we compute the change in the frequency of each SOM
174 node in low-flow years relative to the frequency of this SOM node in normal years. We then
175 draw the same number of low-flow years from normal years with a 1000-iteration bootstrap
176 resampling and compute the frequency change of each SOM node in sampled years relative to
177 the 'normal' years as a background reference. The departure of low-flow SOM frequency
178 changes from the resampled distribution of normal frequency changes is then used to test
179 whether the frequency shifts of SOM patterns in low-flow years are unusual compared to the
180 background state. The SOM methodology avoids information loss common in composite
181 averaging techniques (Kohonen, 1990; Sheridan and Lee, 2011)) and provides critical
182 information surrounding the temporal shifts in tropical Pacific oceanic forcing during low-flow
183 years in the LENS2 dataset.

184 3 Results & Discussion

185 3.1 Historical trends of Mississippi River low-flows

186 The severity and duration of low-flows on the Mississippi River at Vicksburg has decreased from
187 the mid-20th century to present (Fig. 2). Both annual minimum discharge (Q_{\min}) and stage (H_{\min})
188 gradually increased over water years 1950–2022, with the largest increases observed between
189 1950–1980 (Fig 2a) during the rapid expansion of reservoirs within the Mississippi River basin
190 (Smith and Winkley 1996; Remo *et al* 2018). Parallel trends in discharge and stage minima, as
191 well as the ratio of annual minimum to mean discharge (Q_{\min}/Q_{mean}), imply that these increases
192 primarily reflect an increase in low-water discharge, while aggradation of the river bed around
193 Vicksburg likely plays a secondary influence (Harmar *et al* 2005; Wang and Xu 2018). The
194 duration of low stage events (i.e., number of days < 1.5 m stage) has also declined over the
195 period of analysis (Fig. 2b), where the duration of low-flow events in water years 1954 and 1964

196 exceeded 150 days, while the longest duration low-flow events of the 21st century (2006 and
 197 2012) were less than 100 days. These observed trends in river discharge and stage are
 198 consistent across multiple gages of the lower Mississippi River and its tributaries (Turner 2022)
 199 and have previously been attributed through statistical analyses of stream gage records to the
 200 establishment of reservoirs throughout the basin during the mid-20th century and geomorphic
 201 adjustment of the channel to river engineering infrastructure (Jacobson & Galat, 2008; Remo *et*
 202 *al* 2018). The tendency for reservoirs to reduce the severity and duration of low-flows is widely
 203 observed on other regulated rivers (Smakhtin 2001; Verbunt *et al* 2005; Döll *et al* 2009;
 204 Tijdeman *et al* 2018; Brunner *et al* 2019; Brunner and Naveau 2022), and reflects the ability of
 205 dams to gradually release water stored in reservoirs downstream during hydrologic drought.



206
 207 **Figure 2.** Historic trends in lower Mississippi River low-flows: (a) annual minimum discharge
 208 (Q_{min} ; blue), annual minimum stage (H_{min} ; green), and ratio of annual minimum discharge to
 209 annual mean discharge (Q_{min}/Q_{mean}) for water years 1950–2022 showing corresponding loess
 210 curve (lines) and reservoir expansion periods after Remo *et al* (2018), with daily stage and
 211 discharge values for Oct. 24, 2022 also shown; (b) number of low-stage (< 1.5 m) days in a
 212 water year for water years 1950–2022, with years of anomalously high duration noted that
 213 exceed $+1\sigma$ of a linear regression (dashed line); (c) mean soil moisture anomalies (CPC v2) for
 214 the month of minimum stage in 1954, 1964, 1977, 1988, 2000, 2006, and 2012.

215
 216 In the context of increasing annual discharge and stage minima since the mid-20th century, the
 217 low-flow event of 2022 is of moderate severity relative to other historical low-flow events (Fig. 2).
 218 The discharge observed at Vicksburg during the nadir of the 2022 event on October 23 (~5200

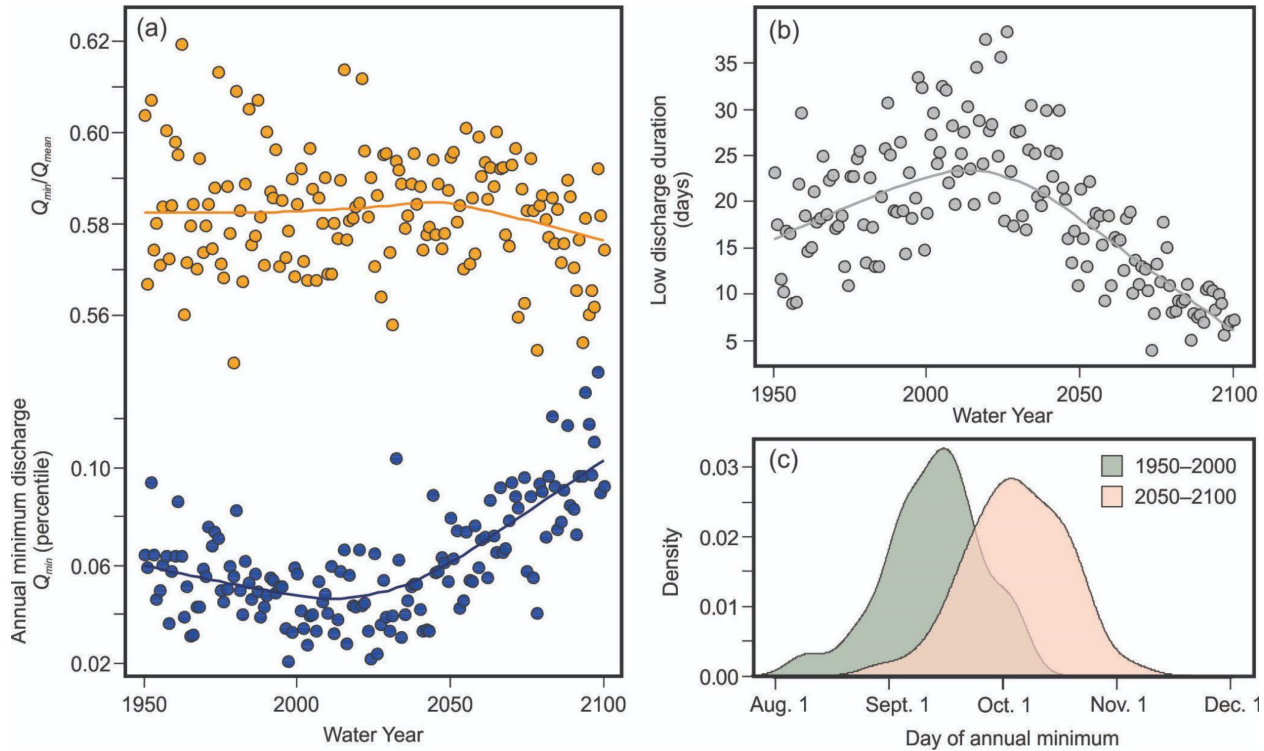
219 m^3/s) is lower than annual minima during other recent low-flow events in 2012 and 2006 (5650
220 and 5858 m^3/s , respectively), but not as severe as annual minima in 1988, 1964, and 1954
221 (3900, 3570, and 3850 m^3/s , respectively) during and shortly after the rapid expansion of
222 reservoirs (Fig. 2a). River stage minima follow a similar trajectory, where October 2022 stages
223 are higher than annual minimum stages during other low-flow events, particularly those prior to
224 1980. The severity of the 2022 low-flow event relative to other historic low-flow events within our
225 period of analysis may differ at other reaches of the Mississippi River, but the trend towards
226 increasing magnitudes of annual discharge minima observed at multiple gages across the basin
227 (Remo *et al* 2018; Turner 2022) implies that the 2022 event is of moderate severity within this
228 historical frame of reference. The pattern of soil moisture anomalies associated with historical
229 low-flow events (Fig. 2c) is consistent with those of the 2022 event (Fig. 1a), supporting our
230 assertion that the historical trend towards decreasing severity of low-flow events primarily
231 reflects management of the Mississippi River and its watershed.

232 3.2 Simulations of historic and projected low-flows

233 To isolate the influence of hydroclimatic change on lower Mississippi River discharge minima
234 from river management practices, we examine simulations of lower Mississippi River discharge
235 in the LENS2 dataset which uses historic and projected (SSP3-7.0 scenario) radiative forcing
236 but does not account for the influence of reservoirs and other river engineering infrastructure on
237 streamflow (Fig. 3). In the LENS2 dataset, the ensemble mean is composed of 40 individual
238 ensemble members, and should primarily reflect the response of the discharge to external
239 forcing because this external forcing is common across all ensemble members. Internal
240 variability is simulated in individual ensemble members, and the ensemble mean minimizes (but
241 does not remove) the influence of internal variability. The ensemble mean of simulated annual
242 minima (Q_{\min}) diverges from observations, declining between 1950–2020 before increasing
243 abruptly through to the end of the 21st century, while the ratio of Q_{\min}/Q_{mean} is stable through the
244 simulation until declining after 2050 (Fig. 3a). The duration of simulated low-discharge events
245 (number of days ≤ 0.05 percentile) follows a similar trajectory, increasing from a mean of 16 to
246 22 days between 1950–2020 before declining such that low-discharge events last <10 days by
247 the end of the 21st century (Fig. 3b). The moderate influence of historic anthropogenic forcing on
248 Mississippi River streamflow in the LENS2 dataset is consistent with other model simulations
249 (Tao *et al* 2014; Dunne *et al* 2022), implying that external forcing of the late 20th and early 21st
250 century has exerted a minor influence on streamflow during this time. Thus, we assert that the
251 divergence of simulated and observed trends during the historic period — where stream gage
252 data document increases in annual minima between 1950–2020 (Fig. 2a) while simulations
253 predict decreases in Q_{\min} during this same period (Fig. 3a) — primarily reflect the influence of
254 reservoirs and other river infrastructure that are not included in the CESM2 simulations. The
255 observed increase in Q_{\min} between 1950–2020 (slope of linear regression=39.77%) is well
256 outside the range of slopes simulated in LENS2 over the same time period ($\bar{x}=-4.89\%$,
257 $\sigma=11.77\%$), implying that observed trends are also not primarily driven by internal variability
258 (Fig. S3). Our approach, comparing trends in the ensemble mean of simulations without
259 reservoirs to trends observed in stream gage data, provides support to the hypothesis that
260 reservoirs play a critical role in regulating Mississippi River streamflow to reduce the severity of
261 low-flow events.

262
 263 Projections of Mississippi River discharge under a high emissions scenario show that the
 264 severity, duration, and seasonality of low-flows shifts during the mid- and late-21st century (Fig.
 265 3). Between 2050 and 2100, the ensemble mean of annual minima increases by ~60% while the
 266 ratio of annual minimum to mean discharge (Q_{\min}/Q_{mean}) decreases as a result of larger
 267 increases in mean and peak annual flows (Dunne et al 2022; Fig. 3a). The duration of low-flow
 268 events mirrors these trends, with a ~70% decline in the number of low-flow days between 2050
 269 and 2100 (Fig. 3b). The timing of low-flows also shifts ~20 days later in the year between the
 270 late-20th and late-21st centuries, such that simulated annual minima from 1950–2000 occur
 271 between Aug. 28–Oct. 1 (0.1 and 0.9 percentiles; median=Sept. 14) but shift to Sept. 19–Oct.
 272 20 (median=Oct. 4) between by 2050–2100 (Fig. 3c). A projected shift towards higher, shorter,
 273 and later low-flows under a high emissions scenario harbors important implications for the
 274 economic consequences of low-flow events, reducing their impact on shipping by alleviating
 275 their severity and shifting them further from fall harvest of row crops currently planted in the
 276 midwestern United States. We caution that although the trends in discharge we observe in the
 277 CESM2 LENS2 simulations are broadly consistent with other model projections (Tao et al 2014;
 278 Lewis et al 2019; Dunne et al 2022), simulations of Mississippi River discharge are sensitive to
 279 the model and emissions scenario used, and do not include the influence of river management
 280 practices or the geomorphic adjustments that arise from those management practices.

281
 282



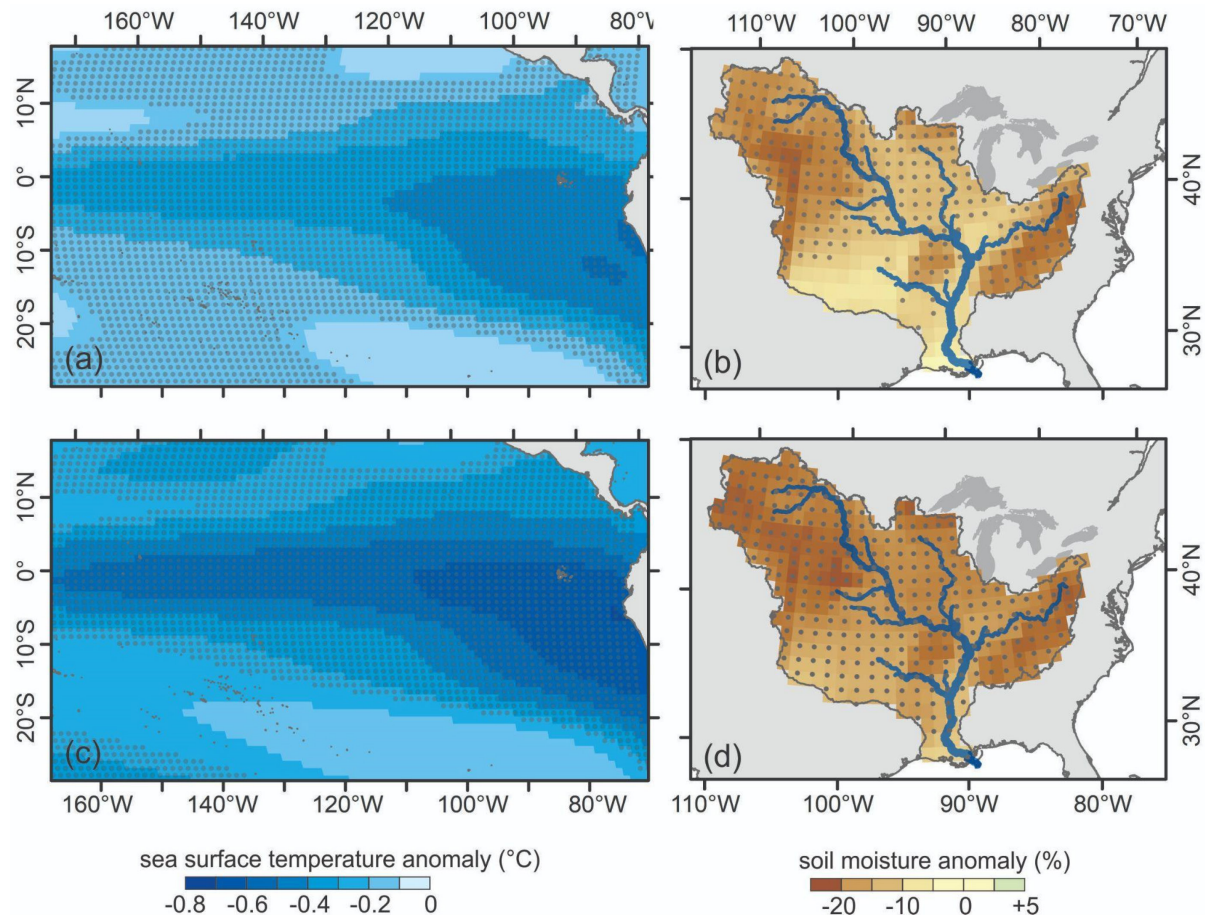
283

284 **Figure 3.** Simulations of historic and projected (SSP3-7.0) trends in lower Mississippi River low-
 285 flows using CESM2 large ensemble (LENS2) ensemble mean: (a) annual minimum discharge
 286 (Q_{\min} ; blue) as a percentile of all values in the ensemble member, and ratio of annual minimum
 287 discharge to annual mean discharge (Q_{\min}/Q_{mean}) for the period 1950–2100 showing

288 corresponding loess curves (lines); (b) number of low discharge days (lowermost 5% of daily
289 discharge values) for the period 1950–2100; (c) timing of annual minimum for the late 20th
290 (1950–2000) and late 21st centuries (2050–2100).
291

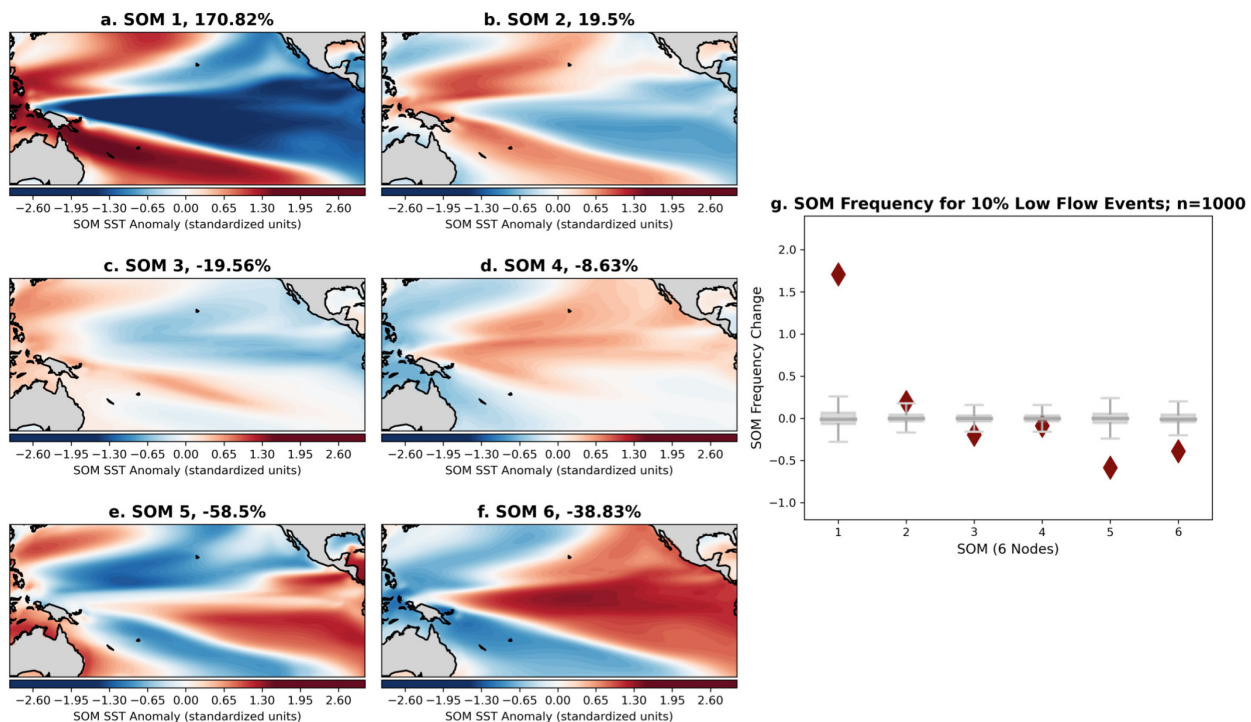
292 3.3 Hydroclimatic mechanisms of low-flows

293 The relatively small number of observed low-flow events since the mid-20th century, together
294 with the confounding influence of reservoir operations, limit the statistical power of the
295 observational record to assess the influence of ENSO on low-flow events (Fig. 1). However, the
296 LENS2 simulations produced by CESM2 — which reproduces hydroclimatic teleconnections
297 associated with ENSO reasonably well (Capotondi *et al* 2020; Danabasoglu *et al* 2020) —
298 bolsters the sample size, and allows us to extend prior work analyzing the role of ENSO-related
299 variability on Mississippi River discharge (Twine *et al* 2005; Liang *et al* 2014; Munoz and Dee,
300 2017; Munoz *et al* 2022; Luo *et al* 2023) to evaluate the correspondence of La Niña events to
301 low-flow events.



302
303 **Figure 4.** Simulations from CESM2 large ensemble (LENS2) for the period 1930–2100 of (a)
304 sea surface temperature anomalies and (b) soil moisture anomalies, expressed as a percent
305 difference of the interquartile range, of the water year associated with the lowest 1% of
306 discharge events ($n=90$), and (c) sea surface temperature anomalies and (d) soil moisture
307 anomalies of the water year associated with the lowest 10% of discharge events ($n=900$) on the

308 lower Mississippi River at Vicksburg. Stippling shows significance of the anomalies via
 309 bootstrapping at the 95% level.
 310
 311 We use the LENS2 simulations to examine the role of tropical Pacific sea surface temperature
 312 and soil moisture anomalies in low-flow events over the period 1930–2100, and find support for
 313 the hypothesis that the El Niño-Southern Oscillation (ENSO) modulates soil moisture and lower
 314 Mississippi River discharge (Fig. 4). In the year of the lowest simulated discharge events ($\leq 1\%$;
 315 $n=90$ years), the composite mean of sea surface temperature anomalies in the eastern
 316 equatorial Pacific are -0.6 to -0.4°C (Fig. 4a), and strongly resembles the cold tongue
 317 characteristic of La Niña events (Philander, 1985). Simulated low-flow extremes also coincide
 318 with negative soil moisture anomalies across the Mississippi River basin (Fig. 4b). Similar and
 319 more pronounced patterns emerge for sea surface temperature (Fig 4c) and soil moisture
 320 anomalies (Fig. 4d) for the lower 10% of simulated discharge events ($\leq 10\%$; $n=900$ years). The
 321 influence of ENSO on soil moisture and streamflow within the Mississippi River basin is
 322 documented in observations, reanalysis, and model simulations including CESM (Munoz and
 323 Dee 2017; Munoz et al 2018; Luo et al 2023), where La Niña conditions result in the poleward
 324 displacement of the polar jet and reduce precipitation and soil moisture across the lower
 325 Mississippi River valley and its western tributaries including the Arkansas and Missouri Rivers
 326 (Ropelewski and Halpert 1986; Hoerling and Kumar 1997; Twine et al 2005; Luo et al. 2023).
 327 We include both the historical and projected simulations in this analysis to increase sample size,
 328 but this is sensitive to both internal climate variability and longer-term climate change.



329
 330 **Figure 5:** Self organizing map (SOM) and frequency analysis for the lowest 10% flow years on
 331 the lower Mississippi River in the CESM2 LENS2 dataset with: (a) through (f) showing SOM
 332 node spatial patterns 1 through 6 of SST anomalies in standardized units, with panel label
 333 indicating the percent change in the frequency of that node during low-flow years relative to its

334 frequency in normal years (25-75%); (g) the change in SOM node frequencies during the 10%
335 lowest flow years ($n=900$ years), where frequency changes of SOM nodes in low-flow events
336 are shown as red diamonds and gray box-plot show background event frequency changes
337 established via resampling with $n=1000$ iterations in normal years.

338
339 To further examine the influence of tropical Pacific sea surface temperature patterns on
340 Mississippi River low-flow events, we applied Self Organizing Maps (SOMs) to the CESM2
341 LENS2 dataset (Fig. 5). Our analysis, based on labeling each year's sea surface temperature
342 field to one of six SOM map nodes of closest resemblance, shows that the lowest 10% of
343 simulated discharges are associated with SOM 1 (Fig. 5a) and SOM 2 (Fig. 5b) which feature
344 negative sea surface temperature anomalies across the eastern equatorial Pacific that closely
345 resemble La Niña conditions (Philander 1985). In contrast, warmer sea surface temperatures
346 across this region are shown in SOM 5 (Fig. 5e) and SOM 6 (Fig. 5f), and the frequencies of
347 these El Niño-like conditions decrease during Mississippi River low-flows (Fig. 5g). An additional
348 test examining only the lowest 1% flow years confirms these results, where the frequency of
349 SOM1 increases by 381%, indicating a strong increase in the frequency of tropical Pacific
350 cooling during the lowest-flow years (Fig. S4). We also examine how the frequency of the SOMs
351 for the lowest 10% of events differ against a resampling of the background in all years, and
352 show that the frequency of strong equatorial Pacific cooling associated with SOM 1 is
353 significantly greater, while El Niño conditions associated with SOMs 5 and 6 are significantly
354 less frequent, during low-flow extremes (Fig. 5g). Taken together, the coupled composite SST
355 and soil moisture anomaly maps for low-flow events (Fig. 4) are consistent with shifts in the
356 frequency of SOMs associated with these same events (Fig. 5). These analyses provide strong
357 support for tropical Pacific modulation of low-flow events on the lower Mississippi River.

358 The projected decrease in low-flow severity and duration in the LENS2 simulations (Fig. 3) is
359 consistent with projections of sea surface temperature warming in the central and eastern
360 tropical Pacific simulated by coupled climate models in the 21st century (e.g., Collins et al. 2010;
361 Xie et al. 2010; Stevenson 2012; Cai et al. 2015; Zheng et al. 2016; Arias et al. 2021). The
362 CESM2 LENS2 simulations are no exception, and show pronounced sea surface temperature
363 warming across the tropical Pacific during the 21st century (Figure S5). These projected
364 changes in mean sea surface temperatures (i.e., warmer tropical Pacific background state), or
365 changes to the variability of ENSO, likely plays a role in modulating the severity and duration of
366 low-flow events on the lower Mississippi River, and provides an example of how changes in
367 mean ocean state may alter streamflow of a major river system.

368
369 We acknowledge important caveats in our use of the CESM2 LENS2 dataset to evaluate the
370 role of tropical Pacific sea surface temperatures on lower Mississippi River discharge. First, we
371 rely on a single model (CESM2) albeit with a large ensemble of 50 ensemble members. Biases
372 in the model's representation of tropical Pacific sea surface temperature and air-sea fluxes are
373 well documented, and indicate that ENSO variance in CESM2 is exaggerated relative to
374 observations (Capotondi et al. 2020; Chen et al. 2021). Teleconnections linking tropical Pacific
375 sea surface temperature forcing to North American precipitation may be too strong in CESM2,
376 partially biasing our results with respect to spatial patterns in soil moisture anomalies. Our use

377 of SOMs, however, which rely solely on the frequency of sea surface temperature patterns in
378 relation to low-flow events, provide evidence consistent with observations (Fig. 1) and simulated
379 anomalies (Fig. 4) that supports a broader hypothesis placing importance of ENSO variability on
380 Mississippi River discharge.

381 4 Conclusions

382
383 Given recent disruptions to riverine transportation on the Mississippi River as a result of low
384 river levels, here we combined observational and simulated datasets to investigate: (i) historical
385 trends in low-flows, (ii) projected trends in low-flows under a moderate-high emissions scenario
386 (SSP3-7.0), and (iii) the role of climate variability, namely ENSO, on low-flow occurrence.
387 Stream gage records from the Mississippi River at Vicksburg show that low-flows, measured in
388 terms of minimum annual stage, minimum annual discharge, and duration of low-stages, have
389 gradually become less severe since 1950, with the largest change between 1950–1980
390 coinciding with the establishment of upstream reservoirs (Fig. 2). In this context, the 2022 low-
391 flow event was less severe than several annual discharge and stage minima of the mid- and
392 late-20th century. We then use earth system model simulations from the CESM2-LENS2 dataset
393 to evaluate the response of Mississippi River low-flows to historic and projected changes in
394 climate, and show that low-flows are projected to become less severe in terms of discharge and
395 duration through to the end of the 21st century (Fig. 3). Finally, we extend prior work examining
396 the role of the El Niño-Southern Oscillation (ENSO) on Mississippi River streamflow to show
397 that La Niña conditions are strongly associated with low-flow events (Fig. 4).
398

399 Our findings provide broader context for the 2022 Mississippi River low-flow event, and support
400 the hypothesis that water resources management — particularly the expansion of artificial
401 reservoirs and the MR&T system during the mid-20th century — exert a strong influence on the
402 severity of low-flows on a major commercial waterway. Further, we clarify how climate change
403 (i.e., anthropogenic forcing) and a dominant mode of climate variability (ENSO) influence the
404 properties and probability of Mississippi River low-flows. Our work implies that La Niña
405 conditions increase the likelihood of low-flows on the lower Mississippi River. Given advances in
406 the seasonal predictability of ENSO (Wu *et al* 2021), we anticipate these findings will aid
407 reservoir operations to reduce the negative impacts of low river levels on river transport.

408 Acknowledgments

409 This project was supported by grants to S.E.M and S.G.D. from the US National Science
410 Foundation (EAR-1804107, EAR-2147781, and EAR-2147782). The authors thank Nathan
411 Steiger for sharing and providing guidance for the Self Organizing Map (SOM) code used in
412 Steiger *et al.* (2019).

413 References

414 Arias, Paola, Nicolas Bellouin, Erika Coppola, Richard Jones, Gerhard Krinner, Jochem
415 Marotzke, Vaishali Naik, et al. 2021. "Climate Change 2021: The Physical Science Basis.

416 Contribution of Working Group I to the Sixth Assessment Report of the Intergovernmental Panel
417 on Climate Change; Technical Summary." In , edited by Valérie Masson-Delmotte, Panmao
418 Zhai, Anna Pirani, S. L. Connors, C. Péan, S. Berger, N. Caud, et al. <https://elib.dlr.de/137584>.

419 Branstetter, M. L. 2001. "Development of a Parallel River Transport Algorithm and Applications
420 to Climate Studies."
421 <https://search.proquest.com/openview/226236cbd3a489d8b19f996b657d7886/1?pq-origsite=gscholar&cbl=18750&diss=y>.

423 Brunner, M. I., Farinotti, D., Zekollari, H., Huss, M., & Zappa, M. (2019). Future shifts in extreme
424 flow regimes in Alpine regions. *Hydrology and Earth System Sciences*, 23(11), 4471-4489.

425 Brunner, M. I., & Naveau, P. (2022). Disentangling natural streamflow from reservoir regulation
426 practices in the Alps using generalized additive models. *Hydrology and Earth System Sciences
427 Discussions*, 1-17.

428 Cai, Wenju, Agus Santoso, Guojian Wang, Sang-Wook Yeh, Soon-II An, Kim M. Cobb, Mat
429 Collins, et al. 2015. "ENSO and Greenhouse Warming." *Nature Climate Change* 5 (9): 849–59.

430 Camillo, C. A., & M. T. Pearcy. 2004. Upon their shoulders: a history of the Mississippi River
431 Commission from its inception through the advent of the modern Mississippi River and
432 tributaries project. Mississippi River Commission, Vicksburg.

433 Capotondi, A., C. Deser, A. S. Phillips, Y. Okumura, and S. M. Larson. 2020. "ENSO and Pacific
434 Decadal Variability in the Community Earth System Model Version 2." *Journal of Advances in
435 Modeling Earth Systems*. <https://doi.org/10.1029/2019ms002022>.

436 Chen, H. C., Fei-Fei-Jin, Zhao, S., Wittenberg, A. T., & Xie, S. (2021). ENSO dynamics in the
437 E3SM-1-0, CESM2, and GFDL-CM4 climate models. *Journal of Climate*, 34(23), 9365-9384.

438 Chen, J., & Kumar, P. (2002). Role of terrestrial hydrologic memory in modulating ENSO
439 impacts in North America. *Journal of Climate*, 15(24), 3569-3585.

440 Collins, Mat, Soon-II An, Wenju Cai, Alexandre Ganachaud, Eric Guilyardi, Fei-Fei Jin, Markus
441 Jochum, et al. 2010. "The Impact of Global Warming on the Tropical Pacific Ocean and El
442 Niño." *Nature Geoscience* 3 (6): 391–97.

443 Danabasoglu, G., J-F Lamarque, J. Bacmeister, D. A. Bailey, A. K. DuVivier, J. Edwards, L. K.
444 Emmons, et al. 2020. "The Community Earth System Model Version 2 (CESM2)." *Journal of
445 Advances in Modeling Earth Systems* 12 (2). <https://doi.org/10.1029/2019ms001916>.

446 Dee, Sylvia G., and Nathan J. Steiger. 2022. "ENSO's Response to Volcanism in a Data
447 Assimilation-based Paleoclimate Reconstruction over the Common Era." *Paleoceanography
448 and Paleoclimatology* 37 (3). <https://doi.org/10.1029/2021pa004290>.

449 Döll, P., Fiedler, K., & Zhang, J. (2009). Global-scale analysis of river flow alterations due to

450 water withdrawals and reservoirs. *Hydrology and Earth System Sciences*, 13(12), 2413-2432.

451 Dunne, K. B. J., Dee, S. G., Reinders, J., Muñoz, S. E., & Nittrouer, J. A. (2022). Examining the
452 impact of emissions scenario on lower Mississippi River flood hazard projections. *Environmental
453 Research Communications*, 4(9), 091001.

454 Fan, Y., & Van Den Dool, H. (2004). Climate Prediction Center global monthly soil moisture data
455 set at 0.5 resolution for 1948 to present. *Journal of Geophysical Research: Atmospheres*,
456 109(D10).

457 Philander, G.S. 1989. *El Niño, La Niña, and the Southern Oscillation*. Academic Press.

458 Hoerling, Martin P., and Arun Kumar. 1997. "Why Do North American Climate Anomalies Differ
459 from One El Niño Event to Another?" *Geophysical Research Letters* 24 (9): 1059–62.

460 Boyin Huang, Peter W. Thorne, Viva F. Banzon, Tim Boyer, Gennady Chepurin, Jay H.
461 Lawrimore, Matthew J. Menne, Thomas M. Smith, Russell S. Vose, and Huai-Min Zhang (2017):
462 NOAA Extended Reconstructed Sea Surface Temperature (ERSST), Version 5. NOAA National
463 Centers for Environmental Information. doi:10.7289/V5T72FNM.

464 Harmar, O. P., Clifford, N. J., Thorne, C. R., & Biedenharn, D. S. (2005). Morphological changes
465 of the Lower Mississippi River: geomorphological response to engineering intervention. *River
466 Research and Applications*, 21(10), 1107-1131.

467 Horton, Daniel E., Nathaniel C. Johnson, Deepti Singh, Daniel L. Swain, Bala Rajaratnam, and
468 Noah S. Diffenbaugh. 2015. "Contribution of Changes in Atmospheric Circulation Patterns to
469 Extreme Temperature Trends." *Nature* 522 (7557): 465–69.

470 Huang, B., Thorne, P. W., Banzon, V. F., Boyer, T., Chepurin, G., Lawrimore, J. H., ... & Zhang,
471 H. M. (2017). Extended reconstructed sea surface temperature, version 5 (ERSSTv5):
472 upgrades, validations, and intercomparisons. *Journal of Climate*, 30(20), 8179-8205.

473 Jacobson, R. B., & Galat, D. L. (2008). Design of a naturalized flow regime—an example from
474 the lower Missouri River, USA. *Ecohydrology: Ecosystems, Land and Water Process
475 Interactions, Ecohydrogeomorphology*, 1(2), 81-104.

476 Johnson, Nathaniel C., Steven B. Feldstein, and Bruno Tremblay. 2008. "The Continuum of
477 Northern Hemisphere Teleconnection Patterns and a Description of the NAO Shift with the Use
478 of Self-Organizing Maps." *Journal of Climate* 21 (23): 6354–71.

479 Kohonen, T. 1990. "The Self-Organizing Map." *Proceedings of the IEEE* 78 (9): 1464–80.

480 Lawrence, D. M., Fisher, R. A., Koven, C. D., Oleson, K. W., Swenson, S. C., Bonan, G., ... &
481 Zeng, X. (2019). The Community Land Model version 5: Description of new features,
482 benchmarking, and impact of forcing uncertainty. *Journal of Advances in Modeling Earth
483 Systems*, 11(12), 4245-4287. Lewis, J. W., Tavakoly, A. A., Martin, C. A., & Moore, C. D. (2019).

484 *Mississippi River and Tributaries future flood conditions*. MRG&P Report No. 28, US Army
485 Corps of Engineers.

486 Li, Hong-Yi, L. Ruby Leung, Augusto Getirana, Maoyi Huang, Huan Wu, Yubin Xu, Jiali Guo,
487 and Nathalie Voisin. 2015. "Evaluating Global Streamflow Simulations by a Physically Based
488 Routing Model Coupled with the Community Land Model." *Journal of Hydrometeorology* 16 (2):
489 948–71.

490 Liang, Y. C., Lo, M. H., & Yu, J. Y. (2014). Asymmetric responses of land hydroclimatology to
491 two types of El Niño in the Mississippi River Basin. *Geophysical Research Letters*, 41(2), 582-
492 588.

493 Liu, Yonggang, and Robert H. Weisberg. 2011. "A Review of Self-Organizing Map Applications
494 in Meteorology and Oceanography." *Self-Organizing Maps: Applications and Novel Algorithm
495 Design* 1: 253–72.

496 Liu, Yonggang, Robert H. Weisberg, and Christopher N. K. Mooers. 2006. "Performance
497 Evaluation of the Self-Organizing Map for Feature Extraction." *Journal of Geophysical
498 Research*. <https://doi.org/10.1029/2005jc003117>.

499 Luo, Xinyue, Sylvia Dee, Trinity Lavenhouse, Samuel Muñoz, and Nathan Steiger. 2023.
500 "Tropical Pacific and North Atlantic Sea Surface Temperature Patterns Modulate Mississippi
501 Basin Hydroclimate Extremes over the Last Millennium." *Geophysical Research Letters* 50 (2).
502 <https://doi.org/10.1029/2022gl100715>.

503 Mallakpour, I., & Villarini, G. (2016). Investigating the relationship between the frequency of
504 flooding over the central United States and large-scale climate. *Advances in Water Resources*,
505 92, 159-171.

506 Munoz, Samuel E., and Sylvia G. Dee. 2017. "El Niño Increases the Risk of Lower Mississippi
507 River Flooding." *Scientific Reports*. <https://doi.org/10.1038/s41598-017-01919-6>.

508 Munoz, S. E., Giosan, L., Therrell, M. D., Remo, J. W., Shen, Z., Sullivan, R. M., & Donnelly, J.
509 P. (2018). Climatic control of Mississippi River flood hazard amplified by river engineering.
510 *Nature*, 556(7699), 95-98.

511 Muñoz, S. E., Hamilton, B., & Parazin, B. (2023). Contrasting Ocean–Atmosphere Dynamics
512 Mediate Flood Hazard across the Mississippi River Basin. *Earth Interactions*, 27(1), e220015.

513 Philander, S. G. H. (1985). El Niño and La Niña. *Journal of Atmospheric Sciences*, 42(23),
514 2652-2662.

515 Pinter, N., Jemberie, A. A., Remo, J. W., Heine, R. A., & Ickes, B. S. (2008). Flood trends and
516 river engineering on the Mississippi River system. *Geophysical Research Letters*, 35(23).

517 Remo, J. W., Pinter, N., & Heine, R. (2009). The use of retro-and scenario-modeling to assess

518 effects of 100+ years river of engineering and land-cover change on Middle and Lower
519 Mississippi River flood stages. *Journal of Hydrology*, 376(3-4), 403-416.

520 Remo, J. W., Ickes, B. S., Ryherd, J. K., Guida, R. J., & Therrell, M. D. (2018). Assessing the
521 impacts of dams and levees on the hydrologic record of the Middle and Lower Mississippi River,
522 USA. *Geomorphology*, 313, 88-100.

523 Rodgers, Keith B., Sun-Seon Lee, Nan Rosenbloom, Axel Timmermann, Gokhan Danabasoglu,
524 Clara Deser, Jim Edwards, et al. 2021. "Ubiquity of Human-Induced Changes in Climate
525 Variability." *Earth System Dynamics* 12 (4): 1393–1411.

526 Ropelewski, C. F., and M. S. Halpert. 1986. "North American Precipitation and Temperature
527 Patterns Associated with the El Niño/Southern Oscillation (ENSO)." *Monthly Weather Review*
528 114 (12): 2352–62.

529 Sheridan, S. C., & Lee, C. C. (2011). The self-organizing map in synoptic climatological
530 research. *Progress in Physical Geography*, 35(1), 109-119.

531 Smakhtin, V. U. (2001). Low flow hydrology: a review. *Journal of hydrology*, 240(3-4), 147-186.

532 Smith, L. M., & Winkley, B. R. (1996). The response of the Lower Mississippi River to river
533 engineering. *Engineering Geology*, 45(1-4), 433-455.

534 Steiger, N. J., Smerdon, J. E., Cook, B. I., Seager, R., Williams, A. P., & Cook, E. R. (2019).
535 Oceanic and radiative forcing of medieval megadroughts in the American Southwest. *Science
536 Advances*, 5(7), eaax0087.

537 Stevenson, S. L. 2012. "Significant Changes to ENSO Strength and Impacts in the Twenty-First
538 Century: Results from CMIP5." *Geophysical Research Letters* 39 (17).
539 <https://doi.org/10.1029/2012gl052759>.

540 St. George, S. (2018). Mississippi rising. *Nature* 556: 34-35.

541 Tao, B., Tian, H., Ren, W., Yang, J., Yang, Q., He, R., ... & Lohrenz, S. (2014). Increasing
542 Mississippi river discharge throughout the 21st century influenced by changes in climate, land
543 use, and atmospheric CO₂. *Geophysical Research Letters*, 41(14), 4978-4986.

544 Tijdeman, E., Hannaford, J., & Stahl, K. (2018). Human influences on streamflow drought
545 characteristics in England and Wales. *Hydrology and Earth System Sciences*, 22(2), 1051-1064.

546 Turner, R. E. (2022). Variability in the discharge of the Mississippi River and tributaries from
547 1817 to 2020. *Plos one*, 17(12), e0276513.

548 Twine, Tracy E., Christopher J. Kucharik, and Jonathan A. Foley. 2005. "Effects of El Niño–
549 Southern Oscillation on the Climate, Water Balance, and Streamflow of the Mississippi River
550 Basin." *Journal of Climate* 18 (22): 4840–61.

551 U.S. Army Corps of Engineers (USACE), (2022). RiverGages.com, water levels of rivers and
552 lakes. www.rivergages.com. (Accessed 30 December 2022).

553 U.S. Department of Agriculture (USDA) (2022) Barge Dashboard.URL:
554 <https://agtransport.usda.gov/stories/s/Barge-Dashboard/965a-yzgy/> (Accessed December 30,
555 2022)

556 U.S. Department of Transportation (USDOT) (2022) Low water on the Mississippi slows critical
557 freight flows. URL: <https://www.bts.gov/data-spotlight/low-water-mississippi-slows-critical-freight-flows> (Accessed December 30, 2022)

559 U.S. Geological Survey (USGS), (2022). USGS surface-water data for the nation.
560 https://waterdata.usgs.gov/monitoring-location/07289000/?agency_cd=USGS#parameterCode=00065&period=P7D. (Accessed 30 December 2022).

562 Van der Wiel, K., Kapnick, S. B., Vecchi, G. A., Smith, J. A., Milly, P. C., & Jia, L. (2018). 100-year lower Mississippi floods in a global climate model: Characteristics and future changes.
563 *Journal of Hydrometeorology*, 19(10), 1547-1563.

565 Verbunt, M., Zwaafink, M. G., & Gurtz, J. (2005). The hydrologic impact of land cover changes
566 and hydropower stations in the Alpine Rhine basin. *Ecological modelling*, 187(1), 71-84.

567 Wang, B., and Xu, Y. J. (2018). Decadal-scale riverbed deformation and sand budget of the last
568 500 km of the Mississippi River: Insights into natural and river engineering effects on a large
569 Alluvial River. *Journal of Geophysical Research: Earth Surface*, 123(5), 874-890.

570 Wiman, C., Hamilton, B., Dee, S. G., & Muñoz, S. E. (2021). Reduced lower Mississippi River
571 discharge during the Medieval era. *Geophysical research letters*, 48(3), e2020GL091182.

572 Wu, Xian, Yuko M. Okumura, Clara Deser, and Pedro N. DiNezio. 2021. “Two-Year Dynamical
573 Predictions of ENSO Event Duration during 1954–2015.” *Journal of Climate* 34 (10): 4069–87.

574 Xie, Shang-Ping, Clara Deser, Gabriel A. Vecchi, Jian Ma, Haiyan Teng, and Andrew T.
575 Wittenberg. 2010. “Global Warming Pattern Formation: Sea Surface Temperature and Rainfall.”
576 *Journal of Climate* 23 (4): 966–86.

577 Zheng, Xiao-Tong, Shang-Ping Xie, Liang-Hong Lv, and Zhen-Qiang Zhou. 2016. “Intermodel
578 Uncertainty in ENSO Amplitude Change Tied to Pacific Ocean Warming Pattern.” *Journal of Climate*
579 29 (20): 7265–79.

580

581